

Deployable stabilization mechanisms for endoscopic procedures

T. Ranzani¹, S. Russo¹, F. Schwab², C. J. Walsh¹, R. J. Wood¹

Abstract—Flexible endoscopes are still the gold standard in most natural orifice transluminal endoscopic surgery (NOTES) procedures; however their flexibility (necessary for navigating through the GI tract) limits their capabilities in terms of distal manipulation and stability. We propose a deployable endoscopic add-on aimed at locally counteracting forces applied at the tip of an endoscope. We analyze different designs: a fully soft version and two hybrid soft-folded versions. The hybrid designs exploit either an inextensible structure pressurized by a soft actuator or the stiffness provided by the unfolded “magic cube” origami structure. We focus on the fabrication and experimental characterization of the proposed structures and present some preliminary designs and integration strategies to mount them on top of current flexible endoscopes.

I. INTRODUCTION

The trend towards reducing the invasiveness of surgical procedures has pushed research towards the development of smaller and smarter instrumentation, able to access remote body locations by passing through natural orifices or more convenient access points [1]. Although a variety of flexible instruments have been proposed in literature, the endoscope remains the gold standard for diagnostic and therapeutics procedures in the gastrointestinal (GI) tract. Performing therapeutic procedures such as removal of early stage cancer through a flexible endoscope introduces several challenges in terms of instrument stability and the capability to provide accurate and repeatable dexterous motions at the surgical site [2]. Techniques such as endoscopic submucosal dissection (ESD) have been proposed [3], but they require substantial learning curves mainly due to the lack of distal countertraction [4]. Different strategies have been proposed for augmenting the therapeutic capabilities of endoscopes by developing multitasking endoscopic platforms [5], [6] or add-ons to the endoscope [7]–[10]. However the inherent flexibility of the instrument, which is necessary for navigating the GI tract, represents one of the most limiting factors when trying to perform distal tissue manipulation tasks [2]; the flexural stiffness in particular drops considerably moving farther from the

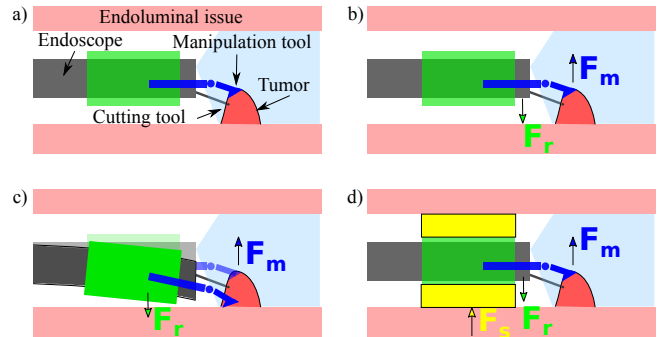


Fig. 1. Illustration of how endoscope flexibility hampers effective force transmission and tissue manipulation tasks a). b) F_m is the force exerted by a tool manipulating tissue and F_r is the reaction force on the endoscope. c) The inherent flexibility of the endoscope causes the instrument to bend during the task. d) The proposed solution with an expandable device mounted around the endoscope.

proximal end [11]. Solutions proposed in literature rely on actively stiffening the endoscope [12] or exploit locally anchored devices with magnets [13]–[15] or mucoadhesives [16]. The effect of endoscope compliance is illustrated in Fig. 1. By locally counteracting the forces applied at the tip we could enable more stable and reliable distal manipulation tasks. To achieve this we propose an actively expandable device fixed at the distal end of conventional endoscopes (see Fig. 1). When trying to expose the tissue with a manipulation tool, as illustrated in Fig. 1 a), the applied force F_m is transmitted to the endoscope (Fig. 1 b)) which may not be able to counteract it properly (F_r) Fig. 1 c). In this paper we propose a system for balancing such effect Fig. 1 d) and stabilize the endoscope by applying a counteracting force F_s . In prior work, expandable balloons have been used as navigation aids for endoscopy [17], [18]. For example, inflatable balloons are commonly used in double balloon endoscopy [19] to assist in traversing sharp curves and collapsed areas in the intestine. Similarly, passive endoscopic add-ons are currently available for improved navigation as well as for more stable distal manipulation [20], [21].

In this paper, we address the issue of improving distal manipulation capabilities with conventional flexible endoscopes. Embedding additional functionality into a system that can be fixed at the tip of the endoscope represents a promising approach for improving current manipulation capabilities without disrupting the current procedure work-flow. We introduce and characterize three different designs: one fully soft, where we

*The authors gratefully acknowledge support from DARPA (award # FA8650-15-C-7548) and the Wyss Institute for Biologically Inspired Engineering.

¹T. Ranzani, S. Russo, C. J. Walsh and R. J. Wood are with the John A. Paulson School of Engineering and Applied Sciences at Harvard University, Cambridge MA 02138, USA, and also with the Wyss Institute for Biologically-Inspired Engineering, Boston, MA 02115, USA [tranzani](mailto:tranzani@seas.harvard.edu), [srusso](mailto:srusso@seas.harvard.edu), [walsh](mailto:walsh@seas.harvard.edu), [rjwood](mailto:rjwood@seas.harvard.edu)

²F. Schwab is with the Swiss Federal Institute of Technology in Zurich, Switzerland schwabf@student.ethz.ch

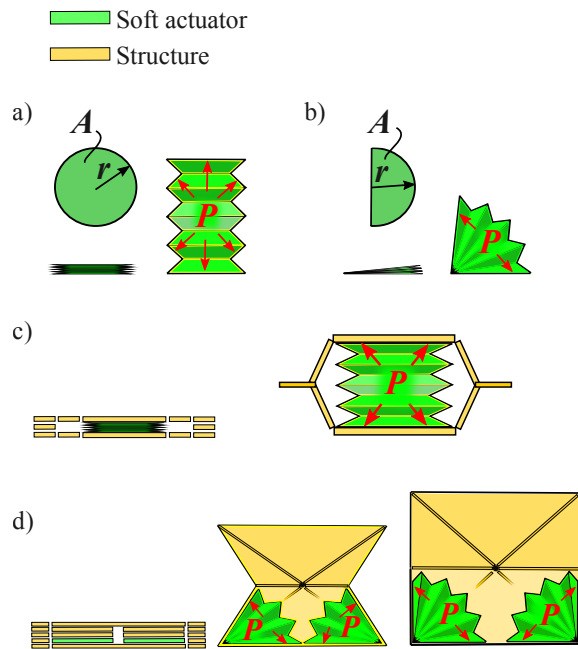


Fig. 2. Overview of the proposed actuators. a) The first design is a soft actuator with a bellows-like structure expanding upon pressurization. b) A similar concept as a) but creating a rotational upon pressurization. c) A second design integrates the soft actuator in a) within a strain limiting structure. d) The third design is an origami “magic cube” that embeds the rotational soft actuator in b).

present a novel 2D manufacturing technique for fabricating soft pneumatic actuators, and two designs exploiting these soft actuators in combination with rigid mechanisms fabricated using the pop-up book MEMS fabrication process [22]. The potential of the pop-up book MEMS manufacturing paradigm for the design of medical devices was introduced in [23]. Integration of inflatable and soft actuators into foldable structures has been investigated in [24] and [25] and the potential for medical applications was explored in [26]. The device can be either fixed at the distal end of the endoscope (in case full stabilization of the instrument is needed) or at the beginning of the steerable section (in case the endoscopist needs to reorient the instrument tip during the procedure). The system can be used in combination with an articulated arm such as the one proposed in [26] or with conventionally used instruments passed through the working channel.

II. DESIGN AND FABRICATION

We propose three different designs which are shown in Fig. 2. The first design is a soft actuator with a bellows-like structure (Fig. 2 a)) that generates a linear motion upon inflation. The second design embeds the soft linear actuator in a strain limiting rigid structure (Fig. 2 c)). The final design exploits soft rotational actuators (Fig. 2 b)) to expand an origami “magic cube” (Fig. 2 d)). The mechanisms are designed to provide a minimum vertical expansion of 13 mm. Integration of multiple mechanisms in a radial configuration around

a 14 mm diameter endoscope will result in a total expanded structure 40 mm in diameter. The geometries are chosen to brace against the inner walls of the large intestine, however the dimensions can be chosen nearly arbitrarily by adjusting the planar geometries of the actuator and structure layers.

A. Design and fabrication of the soft actuators

The soft actuators are fabricated with 50 μm thick Thermoplastic Elastomer - TPE (Fiber Glast, USA) following the process shown in Fig 3a)-c). Different layers of TPE are laser cut with a CO₂ laser and alternated with four laser cut 50 μm thick Teflon layers Fig 3a). Layers of TPE and Teflon are aligned using precision dowel pins. The bottom layer embeds the channel to be connected to a pressure source. The layers of TPE are bonded by heating the laminate at 190 °C for one hour under 0.7 MPa pressure as shown in Fig 3b). The Teflon layers serve to mask areas to selectively bond with the upper or lower TPE layers. The soft actuator is then released from the laminate Fig 3c). Subsequently, a tube with internal diameter of 0.64 mm (Micro Renathane Catheter Tubing, Braintree Scientific, USA) is bonded to the actuator. The same process was used for both the fabrication of the soft linear actuator (Fig. 2 a)) and the soft rotational actuator (Fig. 2 b)). The output force F generated by the actuators can be simply modeled as $F = P \times A$ where P is the input pressure and A is the area indicated in Fig. 2 a) and b).

B. Design and fabrication of the hybrid mechanisms

The strain limiting structure consists of a belt-like mechanism that encapsulates the soft linear actuator (Fig. 2 c)) in order to limit the expansion of the actuator and provide greater stiffness when the pressure is increased. In a second hybrid design, an origami “magic cube” design (Fig. 2 d)) exploits two soft rotational actuators to unfold and extend the structure. When fully expanded, the side walls of the cube provide structural resistance to compression.

Both the strain limiting and the magic cube designs were fabricated by integrating the linear and rotational soft actuators during the lamination process in Fig. 3 d)-e). The fabrication process (bulk laser machining and lamination of the rigid and flexible layers) is based on the *popup book MEMS* process described in [22]. The resulting prototypes are made of three materials: 254 μm glass-reinforced epoxy laminate sheets as structural material, pressure sensitive adhesive (3M[®] 9877), and 25 μm polyimide film as flexible materials. Each layer is laser machined individually using a diode-pumped solid-state (DPSS) laser, realigned using precision dowel pins and laminated together with the soft actuators (Fig. 3 d)). The resulting laminate is laser machined again (Fig. 3 e)) to release the structure from the surrounding bulk material.

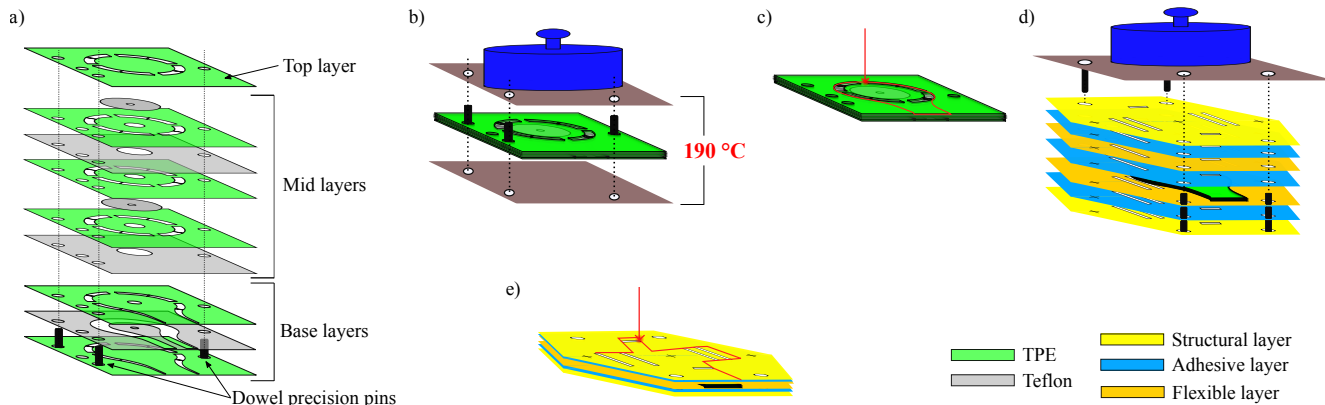


Fig. 3. Fabrication workflow for the proposed mechanisms. The steps necessary to manufacture the soft actuators made from TPE: a) layers of TPE are alternated with Teflon to selectively bond areas of TPE b) under specific temperature and pressure conditions. This structure is subsequently laser machined to release the actuator c). The soft actuator is laminated with the layers forming rigid structures d) and a final laser machining step is performed to release the mechanisms e).

III. EXPERIMENTS

Stress-strain tests on the TPE were performed according to standard ISO 37:2005(E) and repeated on three different samples. The bonding between the TPE layers that constitute the soft actuators was tested to measure the peel strength according to the ASTM standard D903-98(2010) on three samples. The burst pressure of the actuators was measured by pressurizing them to failure. All prototypes were experimentally characterized in terms of blocked force, displacement, and resistance to compression (i.e., stiffness).

A. Soft actuator force characterization

The blocked force of the linear soft actuators was measured by constraining one side and placing the other in contact with a force/torque sensor (Nano 17, ATI Industrial Automation NC, USA). The same setup was used for measuring the block torque on the soft rotational actuators. The internal pressure is recorded using a pressure sensor (BSP B010-EV002-A00A0B-S4,

Balluff, USA). The test was repeated three times on two different actuators.

B. Soft actuator displacement characterization

The linear and angular displacement characterization of the soft actuators is performed by applying increasing pressure and resolving the correspondent displacement visually; the test was repeated three times on two different actuators. Images are taken by placing a camera on a tripod parallel to the actuator and the resulting images are analyzed in Matlab (Mathworks Inc., Natick, MA, USA).

C. Compression tests

In order to assess the capability of the mechanisms to withstand and counteract the forces applied during a procedure with a flexible endoscope, a compression test was performed. All the three designs were tested by placing them in the fully expanded configuration on a rigid plate and imposing a force of 1.5 N with a materials testing machine (Instron), holding the force for 300 s and recording the induced displacement. Each test was repeated three times.

D. Bending stiffness tests

To assess the possibility of improving the flexural stiffness of the endoscope, we integrated the mechanisms at the end of the steerable section (after that point the endoscope tends to bend because of its own weight) of an Olympus CF-100L endoscope. We imposed a 10 mm displacement at the tip with the Instron and recorded the force. The test was repeated in three conditions: 1) rigidly fixing the endoscope (ideal case) as shown in Fig. 4 a), 2) using the strain limiting design on top of a rigid plate (Fig. 4 b)), and 3) using the origami magic cube design on top of a rigid plate (Fig. 4 c). Each test was repeated three times.

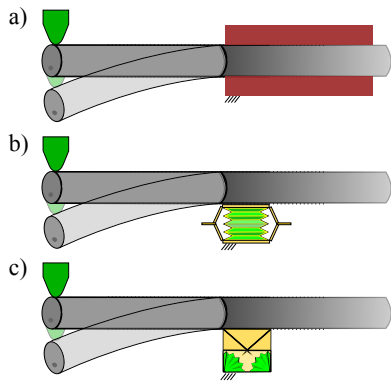


Fig. 4. Experimental setup for the bending stiffness tests. The flexural stiffness of the endoscope was measured in three different conditions: a) fixing the distal part of the endoscope rigidly, b) using the strain limiting structure design, and c) using the magic cube design.

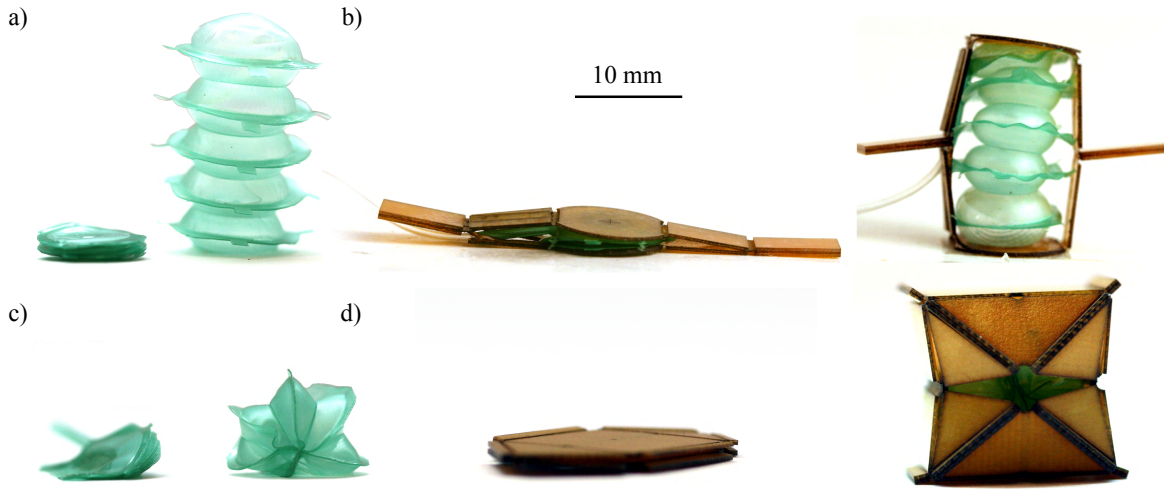


Fig. 5. Fabricated prototypes. a) Soft linear actuator deflated and inflated. b) Soft linear actuator integrated in the strain limiting structure in unactuated and actuated states. c) Soft rotational actuator deflated and inflated. d) Origami magic cube (with two internal soft rotational actuators) in unactuated and actuated states.

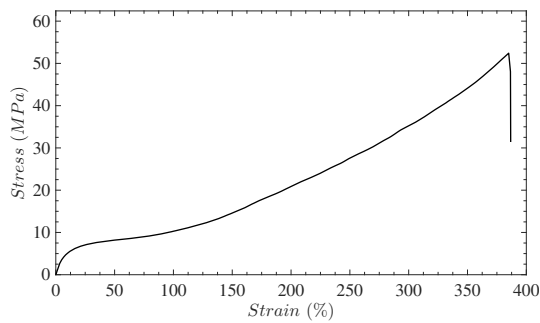


Fig. 6. Stress-strain curve of the TPE.

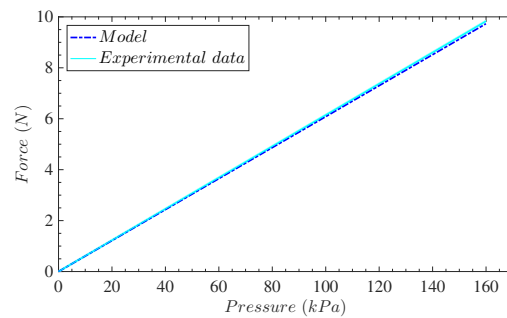


Fig. 7. Blocked force of linear actuators. The dashed line represent the output from the model. The solid line is the mean value and the shaded area represent one standard deviation computed on two three times each.

IV. RESULTS AND DISCUSSION

Prototypes of each actuator type are shown in Fig. 5 in both folded and deployed configurations.

The stress-strain plot of the TPE is shown in Fig. 6, the max stress before failure was 51.2 ± 4 MPa at 387.1 ± 15.8 % strain. The elastic modulus is approximately 10 MPa.

The peel strength for the thermally bonded TPE layers was 0.73 ± 0.02 N/mm (maximum value 0.76 N/mm, minimum value 0.71 N/mm).

The burst pressure for the soft actuators is approximately 104.8 ± 3.2 kPa.

A. Soft actuator force characterization

Results from the blocked force and torque experiments are given in Fig. 7 and Fig. 8 respectively, together with predictions from the simple model in section II-A. Both actuators exhibit a linear trend, with the linear actuator capable of generating up to 9.8 N at 150 kPa. This same test was also performed when the actuator is extended by 13 mm, also in this configuration it was able to generate forces up to 5.2 N at 52 kPa pressure. In addition, these actuators are bidirectional.

By applying vacuum, the soft actuators can be folded back to their original configurations. The forces that the actuators are able to generate when applying negative pressure were approximately 0.5 N. The rotational actuator can provide torques up to 25 mNm at 120 kPa. Also in this case the actuator presents a linear trend and follows the model.

B. Soft actuator displacement characterization

The displacement-pressure curve is shown in Fig. 9. For low pressures (up to 3.5 kPa) the motion is linear – as shown by the dashed line in Fig 9 – as the bellows deform. Increasing the pressure leads to further expansion up to 15 mm due to the strain in the TPE. A similar trend is followed by the rotational actuator (Fig. 10) where for pressure below 4 kPa the trend is linear and angles up to 100° can be reached. Angles up to 156° can be obtained upon additional pressurization.

C. Compression tests

Fig. 11 shows the results of the compression test on the soft linear actuator, the strain limiting structure,

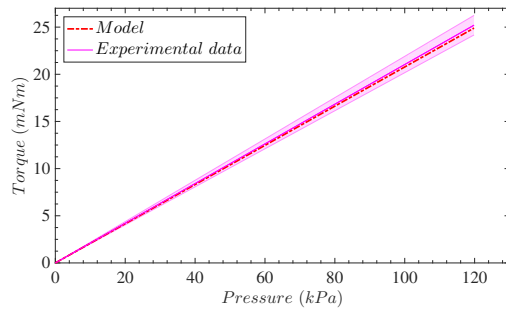


Fig. 8. Blocked torque of rotational actuators. The dashed line represent the output from the model. The solid line is the mean value and the shaded area represent one standard deviation computed on two prototypes, tested three times each.

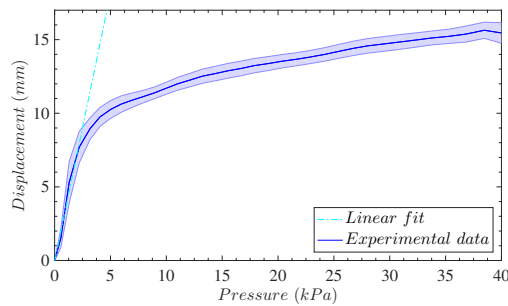


Fig. 9. Displacement characterization of the soft linear actuator. The solid line is the mean value and the shaded area represents one standard deviation computed on two prototypes, tested three times each. The dashed lines represent a linear fit of the experimental data up to 3.5 kPa.

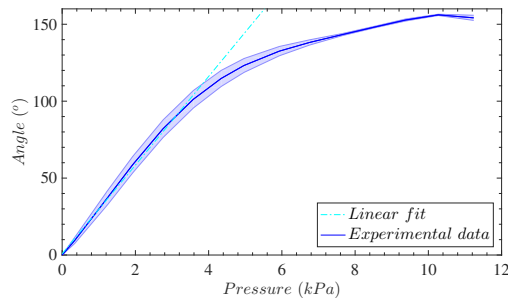


Fig. 10. Angular displacement characterization of the soft rotational actuator. The solid line is the mean value and the shaded area represents one standard deviation computed on two prototypes, tested three times each. The dashed lines represent a linear fit of the experimental data up to 4 kPa.

and the origami magic cube. Both the soft actuator and the strain limiting structure were pressurized at 40 kPa resulting in an initial height of 15 mm. The rotational actuators embedded in the origami magic cube were pressurized until the structure was completely deployed. After an initial transient (necessary for the Instron testing machine to reach the target force value of 1.5 N), all three designs are able to preserve their position and remain stable. The target force was chosen based of force requirements for effective tissue manipulation [27]. The soft linear actuator, due to its compliant nature, experienced an average compression

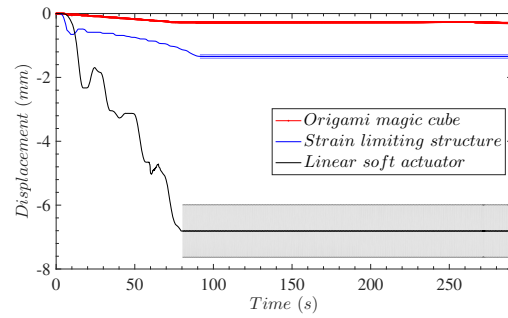


Fig. 11. Plot of the displacement experienced by the soft linear actuator, strain limiting structure, and origami magic cube when 1.5 N force is applied. The solid line is the mean value and the shaded areas represent one standard deviation computed on three repetitions of the test.

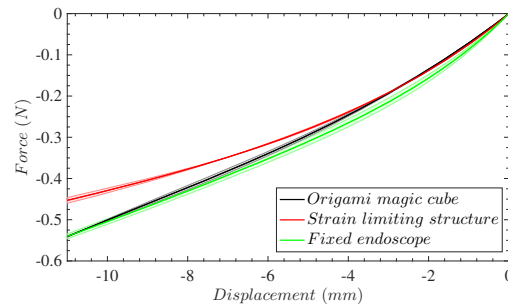


Fig. 12. Results of the flexible endoscope bending tests; comparison between the ideal case of the rigidly constrained endoscope, and the introduction of the strain limiting structure or the origami magic cube. The solid line is the mean value and the shaded area represents one standard deviation computed on three repetitions of the test.

of $6.8 \text{ mm} \pm 1 \text{ mm}$ and presented the largest variability. This would result in large motions during endoluminal tissue manipulation. The hybrid approaches (strain limiting structure and origami magic cube) considerably improved the performances both in terms of compressibility and variability. The strain limiting structure experienced a compression of $1.3 \text{ mm} \pm 0.06 \text{ mm}$ and the origami magic cube underwent a compression of $0.3 \pm 0.01 \text{ mm}$.

D. Bending stiffness tests

The results from the bending tests are reported in Fig. 12. The fixed endoscope represents the best case scenario where the base of the bending section is fully constrained. The origami magic cube design demonstrated the ability to fully restore the stiffness locally, requiring the same force to deflect the tip by the same amount. The strain limiting design is also able to act as fixed point, although for forces higher than 0.3 N it starts to diverge from the ideal case.

E. Fabrication of multiple units and endoscope integration

Given that the fabrication workflow is a parallel process, multiple units can be fabricated in the same laminate; in Fig. 13 a) a laminate embedding seven linear actuators is shown, all actuators share the same

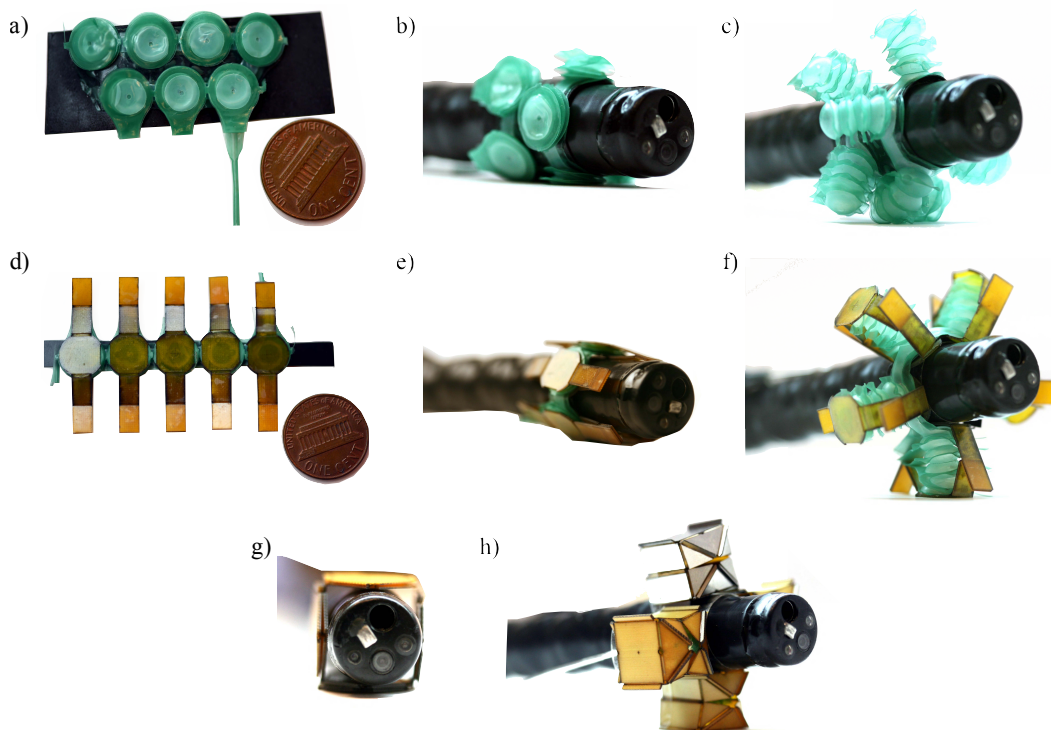


Fig. 13. Integration of the three proposed actuators designs around a flexible endoscope. a) Seven soft linear actuators are interconnected so that they can be inflated with a single tube. b) The actuators are integrated on a sleeve mounded on the endoscope and c) subsequently are inflated, expanding into the bracing structure. d) Similarly, five strain limiting structures are fabricated in a single batch with one channel for inflation, e) positioned around the endoscope, and f) inflated. g) Four origami magic cubes are likewise attached on the outer part of the endoscope and h) their inflation is demonstrated.

inflation channel. Similarly in Fig. 13 d) a composite laminate with strain limiting designs is shown. Both the soft and strain limiting designs can be integrated on a flexible endoscope by wrapping the laminate circumferentially as shown in Fig. 13 b) and e) respectively. In the case of the soft sleeve, the diameter added to the endoscope in the deflated configuration is 1.6 mm. Fig. 13 c) shows a picture of the soft sleeve inflated. In the case of the strain limiting design, the width added to the endoscope diameter is 3.2 mm in the deflated configuration; the inflated configuration is shown in Fig. 13 f). For the origami magic cube design we integrated each cube separately on the endoscope. In the deflated configuration the maximum added dimension to the endoscope diameter is 5 mm and the inflated configuration is shown in Fig. 13 h). Currently the actuators are integrated as discrete elements, which may not be optimal in terms of forming areas of stress concentrations. Future efforts will focus on integrating actuators into a rounded structure coaxial with respect to the endoscope.

V. CONCLUSIONS

In this paper we analyze the possibility of integrating endoscopic add-ons to locally counteract forces applied at the tip of a flexible endoscope without increasing the stiffness of the instrument and thus

its navigation capabilities. We introduce a layer-by-layer manufacturing method for fabricating linear and rotational soft actuators. The stroke of the actuators can be geometrically programmed according to the number of layers. The manufacturing method of the soft actuators doesn't require any adhesives and enables batch manufacturing. The actuators present a linear trend both in force and displacement as long as the deformation is related to the unfolding of the structure. We demonstrate the possibility of integrating the soft actuators into rigid structures to improve their performances, illustrating two different design approaches: a strain-limiting structure and an origami magic cube. All proposed systems are fabricated using materials previously used in the manufacturing of medical devices and are characterized in terms of their capability of withstanding compression forces. The origami magic cube was able to compensate for the highly flexible structure of conventional endoscopes that are particularly compliant after the steerable section. We fabricated multiple prototypes for each design and fixed them on a flexible endoscope. All the designs have a low footprint – adding a maximum of 5 mm to the outer diameter of the endoscope (in their undeployed states) – and can be actively opened and closed several times, paving the way for their use also as navigation

aids. The devices can be mounted at the distal tip of the endoscope or before the bending section depending on the specific application or endoscopist's preference. Mounting them proximal to the steerable section gives the advantage of acting as a local grounding point for being able to apply forces distally in a more reliable and stable way. We focus on the design and characterization of a single expansion device, although we envisage integrating multiple elements radially arranged in order to be able to counteract distal forces independently on the endoscope orientation. The devices can be used in combination with conventional endoscopic instruments that can be passed through the endoscope working channel (which is left free since the proposed designs are conceived to be mounted on the outer part of the endoscope) as well as with manipulation aids such as the multi-articulated arm proposed in [28]. Future work will focus on improving the integration of multiple prototypes in a radial arrangement and embedding them in an external sleeve to reduce potential stress concentration on areas of the GI tract.

ACKNOWLEDGMENT

The authors would like to acknowledge the Wyss Institute for Biologically-Inspired Engineering for their support of this work. The authors would also like to acknowledge DARPA (grant FA8650-15-C-7548). We would also like to thank Daniel Vogt and William White for helping during the fabrication of the actuators.

REFERENCES

- [1] V. Vitiello, Su-Lin Lee, T. P. Cundy, and G.-Z. Yang, "Emerging Robotic Platforms for Minimally Invasive Surgery," *Biomedical Engineering, IEEE Reviews in*, vol. 6, no. c, pp. 111–126, 2013.
- [2] A. Loeve, P. Breedveld, and J. Dankelman, "Scopes Too Flexible...and Too Stiff," *IEEE Pulse*, vol. 1, no. 3, pp. 26–41, 11 2010.
- [3] H. Yamamoto, "Endoscopic submucosal dissection—current success and future directions." *Nature reviews. Gastroenterology & hepatology*, vol. 9, no. 9, pp. 519–29, 6 2012.
- [4] H. Aihara, N. Kumar, M. Ryou, W. Abidi, M. B. Ryan, and C. C. Thompson, "Facilitating endoscopic submucosal dissection: The suture-pulley method significantly improves procedure time and minimizes technical difficulty compared with conventional technique: An ex vivo study (with video)," *Gastrointestinal Endoscopy*, vol. 80, no. 3, pp. 495–502, 2014.
- [5] B. P. M. Yeung and T. Gourlay, "A technical review of flexible endoscopic multitasking platforms," *International Journal of Surgery*, vol. 10, no. 7, pp. 345–354, 1 2012.
- [6] L. L. Swanstrom, "NOTES: Platform development for a paradigm shift in flexible endoscopy." *Gastroenterology*, vol. 140, no. 4, pp. 1150–1154.e1, 2011.
- [7] S. Konishi, S. Sawano, N. Fujiwara, Y. Kurumi, and T. Tani, "Outer shell actuator driving central bending shaft by balloon arrays circumferentially-arranged inside of shell," *TRANSDUCERS 2009 - 15th International Conference on Solid-State Sensors, Actuators and Microsystems*, pp. 53–56, 2009.
- [8] R. Nakadate, S. Nakamura, T. Moriyama, H. Kenmotsu, S. Oguri, J. Arata, M. Uemura, K. Ohuchida, T. Akahoshi, T. Ikeda, and M. Hashizume, "Gastric endoscopic submucosal dissection using novel 2.6-mm articulating devices: an ex vivo comparative and in vivo feasibility study," pp. 820–824, 2015.
- [9] G. P. Mylonas, V. Vitiello, T. P. Cundy, A. Darzi, and G.-Z. Yang, "CYCLOPS: A versatile robotic tool for bimanual single-access and natural-orifice endoscopic surgery," *2014 IEEE International Conference on Robotics and Automation (ICRA)*, pp. 2436–2442, 2014.
- [10] J. B. Gafford, T. Ranzani, S. Russo, H. Aihara, R. J. Wood, C. J. Walsh, and C. Thompson, "Snap-on robotic wrist module for enhanced dexterity in endoscopic surgery," in *2016 IEEE International Conference on Robotics and Automation (ICRA)*. IEEE, 5 2016, pp. 4398–4405.
- [11] D. Hellier, F. Albermani, B. Evans, H. de Visser, C. Adam, and J. Passenger, "Flexural and torsional rigidity of colonoscopes at room and body temperatures," *Proceedings of the Institution of Mechanical Engineers, Part H: Journal of Engineering in Medicine*, vol. 1, no. -1, pp. 1–11, 1 2011.
- [12] A. J. Loeve, O. S. van de Ven, J. G. Vogel, P. Breedveld, and J. Dankelman, "Vacuum packed particles as flexible endoscope guides with controllable rigidity," *Granular Matter*, vol. 12, no. 6, pp. 543–554, 12 2010.
- [13] "Levita Magnetics." [Online]. Available: <http://levita.com/>
- [14] G. Tortora, T. Ranzani, I. De Falco, P. Dario, and A. Menciassi, "A Miniature Robot for Retraction Tasks under Vision Assistance in Minimally Invasive Surgery," *Robotics*, vol. 3, no. 1, pp. 70–82, 3 2014.
- [15] G. Tortora, M. Salerno, T. Ranzani, S. Tognarelli, P. Dario, and A. Menciassi, "A modular magnetic platform for natural orifice transluminal endoscopic surgery," in *2013 35th Annual International Conference of the IEEE Engineering in Medicine and Biology Society (EMBC)*, vol. 2013. IEEE, 7 2013, pp. 6265–6268.
- [16] S. Tognarelli, V. Pensabene, S. Condino, P. Valdastri, A. Menciassi, A. Arezzo, and P. Dario, "A pilot study on a new anchoring mechanism for surgical applications based on mucoadhesives," *Minimally Invasive Therapy & Allied Technologies*, vol. 20, no. 1, pp. 3–13, 2011.
- [17] B. Vucelic, D. K. Rex, R. Pulanic, J. Pfefer, I. Hrstic, B. Levin, Z. Halpern, and N. Arber, "The Aer-O-Scope: Proof of Concept of a Pneumatic, Skill-Independent, Self-Propelling, Self-Navigating Colonoscope," *Gastroenterology*, vol. 130, no. 3, pp. 672–677, 2006.
- [18] W. Grundfest, A. Slatkin, J. Burdick, and W. Grundfest, "The development of a robotic endoscope," *Proceedings 1995 IEEE/RSJ International Conference on Intelligent Robots and Systems. Human Robot Interaction and Cooperative Robots*, vol. 2, pp. 162–171, 1995.
- [19] D.-b. Endoscopy, H. Yamamoto, C. Ell, H. Kita, and A. May, *Video Capsule Endoscopy*, M. Keuchel, F. Hagenmüller, and H. Tajiri, Eds. Berlin, Heidelberg: Springer Berlin Heidelberg, 2014.
- [20] "Aquilant Endoscopy - EndoRings Distal Attachment." [Online]. Available: http://www.aquilantendoscopy.com/products/products{_}detail.asp?subp=products{_}by{_}.all.asp{\&}idProduct=12370
- [21] "ARC Medical." [Online]. Available: <http://www.endocuff.com/>
- [22] J. P. Whitney, P. S. Sreetharan, K. Y. Ma, and R. J. Wood, "Pop-up book MEMS," *Journal of Micromechanics and Microengineering*, vol. 21, no. 11, p. 115021, 2011.
- [23] J. Gafford, T. Ranzani, S. Russo, A. Degirmenci, S. Kesner, R. D. Howe, R. J. Wood, and C. Walsh, "Towards Medical Devices with Integrated Mechanisms, Sensors and Actuators via Printed-Circuit MEMS," *Journal of Medical Devices*, 12 2016.
- [24] X. Sun, S. M. Felton, R. Niiyama, R. J. Wood, and S. Kim, "Self-folding and self-actuating robots: A pneumatic approach," in *2015 IEEE International Conference on Robotics and Automation (ICRA)*. IEEE, 5 2015, pp. 3160–3165.
- [25] L. Paez, G. Agarwal, and J. Paik, "Design and Analysis of a Soft Pneumatic Actuator with Origami Shell Reinforcement," *Soft Robotics*, vol. 3, no. 3, p. soro.2016.0023, 2016.
- [26] S. Russo, T. Ranzani, J. Gafford, C. Walsh, and R. Wood, "Soft pop-up mechanisms for micro surgical tools: Design and characterization of compliant millimeter-scale articulated structures," in *2016 IEEE International Conference on Robotics and Automation (ICRA)*. IEEE, 5 2016, pp. 750–757.
- [27] T. Ranzani, G. Ciuti, G. Tortora, A. Arezzo, S. Arolfo, M. Morino, and A. Menciassi, "A Novel Device for Measuring Forces in Endoluminal Procedures," *International Journal of Advanced Robotic Systems*, p. 1, 2015.
- [28] S. Russo, T. Ranzani, J. B. Gafford, C. J. Walsh, and R. J. Wood, "Soft pop-up mechanisms for micro surgical tools : design and characterization of compliant millimeter-scale articulated structures," *journal of medical devices*, 2016.